Review Article

Lung monitoring with electrical impedance tomography: technical considerations and clinical applications

Vinko Tomicic[1], Rodrigo Cornejo[2]

[1]Jefe Unidad de Cuidados Intensivos Respiratorios, Clínica Indisa, Universidad Andres Bello, Santiago, Chile; [2]Jefe Unidad de Pacientes Críticos, Departamento de Medicina, Hospital Clínico Universidad de Chile, Chile

Contributions: (I) Conception and design: All authors; (II) Administrative support: R Cornejo; (III) Provision of study materials or patients: All authors; (IV) Collection and assembly of data: All authors; (V) Data analysis and interpretation: All authors; (VI) Manuscript writing: All authors; (VII) Final approval of manuscript: All authors.

Correspondence to: Rodrigo Cornejo, MD, FACP. Associate Professor Universidad de Chile, Unidad de Pacientes Críticos, Hospital Clínico Universidad de Chile, Santos Dumont 999, Independencia, Santiago, Chile. Email: racornej@gmail.com; rcornejor@hcuch.cl.

Abstract: In recent years there has been substantial progress in the imaging evaluation of patients with lung disease requiring mechanical ventilatory assistance. This has been demonstrated by the inclusion of pulmonary ultrasound, positron emission tomography, electrical impedance tomography (EIT), and magnetic resonance imaging (MRI). The EIT uses electric current to evaluate the distribution of alternating current conductivity within the thoracic cavity. The advantage of the latter is that it is non-invasive, bedside radiation-free functional imaging modality for continuous monitoring of lung ventilation and perfusion. EIT can detect recruitment or derecruitment, overdistension, variation of poorly ventilated lung units (silent spaces), and pendelluft phenomenon in spontaneously breathing patients. In addition, the regional expiratory time constants have been recently explored.

Keywords: Electrical impedance tomography (EIT); critical care; physiologic monitoring; acute respiratory distress syndrome (ARDS)

Submitted Feb 12, 2019. Accepted for publication Jun 06, 2019.
doi: 10.21037/jtd.2019.06.27
View this article at: http://dx.doi.org/10.21037/jtd.2019.06.27

Introduction

In the critical care scenario, continuous assessment of respiratory status is one of the cornerstones, and imaging, which is considered key for diagnosis and monitoring of lung diseases, is currently being developed in two directions: innovatory and high degree of complexity imaging methods to visualize detailed anatomical lung images to improve our understanding of the disease and the effect of therapeutic strategies; and, easily accessible imaging radiation free techniques that allow continuous and functional respiratory monitoring at the bedside (1). Electrical impedance tomography (EIT), which is part of this second group, is based on the repeated measurement of the surface voltages resulting from a rotating injection of high frequency and low intensity alternating current that circulates between the electrodes located around the chest. The electrodes collect the information on impedance by forming a relative image with respect to a reference. The tissues allow the passage of current with little resistance, however, with gas the opposite occurs. In this way, it is possible to perform a plethysmography of the volume entering upon each inspiration and in each region of interest.

The information obtained through EIT can be analyzed online and offline to detect recruitment, derecruitment, overdistension or variation of poorly ventilated lung units (silent spaces) in response to PEEP changes, and pendelluft phenomenon in spontaneously breathing patients. Recently, regional expiratory time constants in patients with obstructive pulmonary diseases and acute respiratory distress syndrome (ARDS) has been explored, and it may

help to adjust mechanical ventilation in response to the patterns of regional airflow obstruction.

In addition, with this technique it is also feasible to estimate the local lung perfusion and associating these data with the ventilation signal mapping of regional ventilation-perfusion ratios can be provided. Pulmonary conditions are constantly changing and continuous EIT monitoring can be a useful tool for detecting these variations. In this review, we will highlight technical considerations and clinical applications for mechanically ventilated adult patients.

Technical considerations

Basic characteristics of EIT for lung monitoring

Impedance is a physical variable that describes the resistance to the passage of current that an inanimate body (minerals) or a biological tissue (bioimpedance) exerts based on its characteristics. The impedance unit is the ohm (Ω). EIT for lung monitoring is based on the repeated measurement of the surface voltages resulting from a rotating injection of high frequency (50–80 kHz) and low intensity (5–10 mA) alternating current that circulates between the electrodes located around the thorax. The region of electrodes placement should be sensitive to the phenomena of interest. In the 5th to 6th intercostal spaces at the parasternal line allows good representation of impedance changes mainly in the lower lobes of the right and left lungs as well as in the heart region (2). In our experience (and from other authors) with CT and EIT simultaneous acquisitions, the placement of the electrodes belt below the 6th intercostal space limits the quality of the acquisition, because the diaphragm may periodically enter the measurement plane. In contrast, when the electrode plane is located in the 3rd to 4th intercostal spaces, less heart activity will appear. With a computer and 16 or 32 electrodes (with 1 or 2 neutral or reference electrodes) applied to the patient's chest, the bioimpedance signal can be processed, which allows for description of tissue characteristics (conductivity) located in the selected body circumference. The number of electrodes is related to the image resolution. On average, in 16-electrode systems, resolution is 12% of the thoracic diameter for regions in the periphery of the lung and 20% for central regions. In 32-electrode systems, this resolution can be improved to 6–10% of the thoracic diameter (3). All current EIT devices have electrodes arranged in a flexible belt, so the electrodes are fixed to the chest in a short time. The reproducibility of measurements with these new electrode straps has not yet been tested. In the classical study of EIT validation, with conventional ECG electrodes, the bias observed was less than 1% (4). In the cross-sectional plane, the resolution corresponds to approximately 3 cm; while, the spatial resolution in the craniocaudal direction provides a slice thickness of 10 cm (chest mapping). Despite, this thickness differs from whole lung obtained through other images methods, EIT can detect heterogeneities along the gravity axis in different lung diseases. EIT could improve its spatial resolution by increasing the number of electrodes or by improving hardware performance but will never achieve the resolution of CT or MRI (3).

During EIT monitoring, cyclic injections of electrical currents are performed sequentially, usually between all adjacent pairs of electrodes. This means that in a 16-electrode system, the current is injected 16 times during each measurement cycle. During each application, the resulting potential differences are measured between the 13 pairs of passive electrodes. This pattern of current injections and potential difference measurements results in a set of 208 voltages acquired during each cycle. The voltage data obtained on the surface of the body is used to calculate the distribution of electrical impedance within the chest. This process is called image reconstruction, since the calculated regional impedance values can be used to generate cross-sectional images, that is, scans of their thoracic distribution (5). EIT scanning frequencies are high, and in the currently available equipment, sampling rates of 40–50 cycles per second are feasible. These rates of exploration are much higher than the ones used in conventional radiology, like for example, in magnetic resonance imaging and CT scans (6).

Spatial and temporal resolution

Firstly, we must clarify some basic concepts related to EIT. (I) Spatial resolution has to do with the capacity of a sensor to distinguish the smallest object, or in other words, the area represented by a pixel; (II) temporal resolution deals with the frequency with which the sensor registers (25–50 cycles/second). Thus, spatial resolution of CT is much higher than EIT, but temporal resolution of EIT is much higher than in CT or MRI (3); (III) signal to noise ratio: this is the relation between the power of the signal that is transmitted and the power of the noise that corrupts that signal (in decibels).

Image resolution is at its best when more electrodes are used (spatial resolution); nevertheless, with a higher number of electrodes, their proximity increases the signal to noise

ratio, which can interfere in the quality of the signal. It is also necessary to consider the contact impedance, which is the kind occurring (as the name indicates) in the junction between the electrode and the skin (7) (*Table 1*).

The impedance is a mathematically complex number formed by a real part (the resistance) and another virtual one (reactance). If we apply this variable to a biological tissue, we get different resistance to current flow (*Table 2*). However, the figures are not absolute and may vary based on environmental conditions, such as temperature (2).

Table 1 Electrical impedance tomography characteristics

Spatial resolution
Temporal resolution
Signal to noise ratio
Contact impedance

Table 2 Body tissue resistivity to passage of current (50 Hz)

Tissue	Resistivity (Ωm)
Lung during expiration	12.5
Lung during inspiration	25
Blood (50% hematocrit)	1.4–1.7
Cardiac muscle	2.5–5
Skeletal muscle	1.5–5
Liver	8.3
Fat	10–50
Radial bone	160

Electrical impedance distribution

In general, the measurements are based on the application of alternating current through two contiguous electrodes (emitters), while the rest of the electrodes (receivers) pick up the electrical signal. This signal travels through the thorax following pathways that vary based on the shape of the chest wall and the distribution of the obstacles that the intrathoracic structures pose, that is, the electrical potentials that will be picked up on the surface of the chest wall (*Figure 1*). Immediately afterwards, the next pair of electrodes injects the current, and the rest of the electrodes receive the resulting voltage and so on. This information is recorded by a computer. The densities of the tissues determine the electrical potentials that will be measured on the chest surface (*Figure 1*). These potentials are used to obtain the electrical impedance distribution through the use of a reconstruction algorithm that solves the problem of signal non-linearity, which will be explained later.

Each complete round of impedance measurement of the analyzed section is called a cycle. The current tomographs, as mentioned above, usually complete 25–50 cycles per second (temporal resolution), that is, 25 to 50 images per second (*frames or raw images*), and with 16 electrodes, an image of the plane defined by a matrix of 1,024 pixels (spatial resolution) can be generated. The number of frames (or raw images) acquired per second is the *scan rate* of the device. Currently available equipment offers a maximum scan rate of 50 frames per second, which allows the evaluation of lung

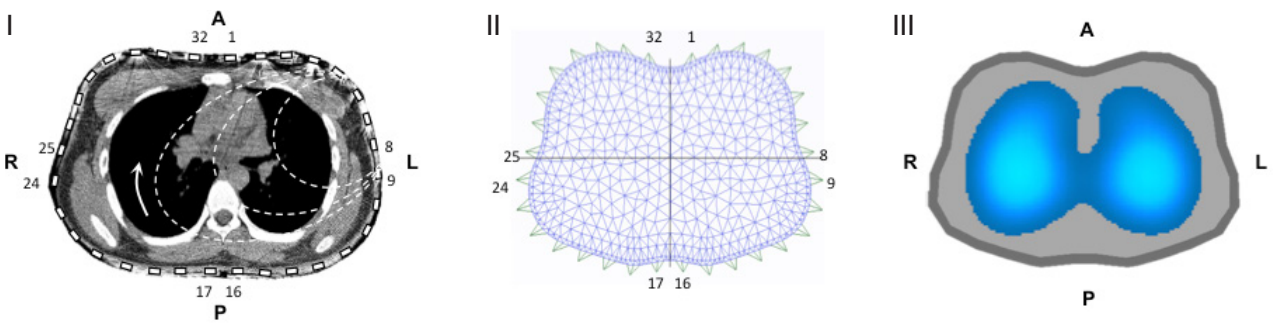

Figure 1 On the left (I), distribution of the electrical signal based on the opposition exerted by each chest structure to the passage of current. On the middle (II), symmetrical distribution of the electrical signal observed in a mesh. The excitatory current is applied consecutively between pairs of adjacent electrodes. After each injection of current, the resulting voltages (U) are measured between the remaining pairs of electrodes. On the right (III), it is shown the image obtained during ventilation trough electrical impedance tomography Enlight 1800 with 32 electrodes (Timpel, Sao Paulo, Brazil). Project FONDECYT 1161510. Cornejo *et al.*

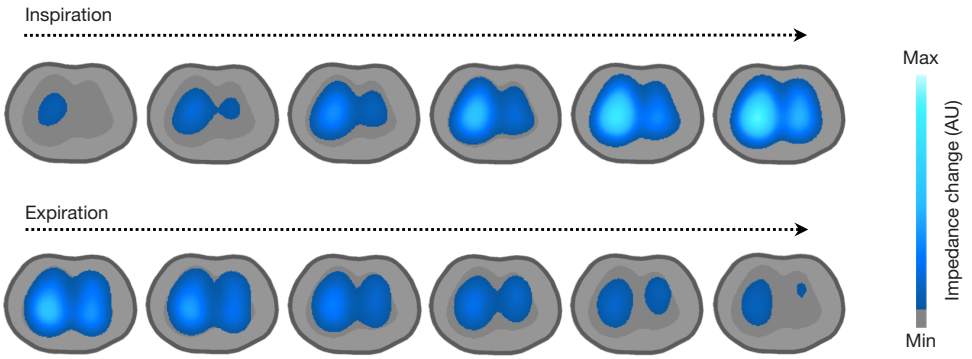

Figure 2 Dynamic images during one respiratory cycle, where inspiration and expiration images were acquired with Electrical Impedance Tomography Enlight 1800 (Timpel, Sao Paulo, Brazil). Right lung is inflated before left lung and left lung become deflated before right lung

function under dynamic conditions (2) (*Figure 2*).

Reconstruction algorithms

For the reconstruction of the information, the change in the relative impedance in each pixel is used. This (dimensionless) value is derived from the difference in tissue impedance between two instants in time or between inspiration and expiration [expressed in arbitrary units (AU)].

The method used to reconstruct the information in images is crucial. The most used clinical method is the *Sheffield backprojection algorithm* and its subsequent modifications (8). The reconstruction algorithms refer to the calculations made by the computer that transform the acquired voltages on the chest surface into an impedance image of a cross section thereof (*Figure 1*). The first algorithm used to generate images of ventilation using EIT was called *backprojection* filter and uses a linear approach to solve the problem of the impedance distribution characteristics. This approach imposes some restrictions in terms of the maximum impedance variation that can be reliably measured. Many other linearized algorithms have been developed in search of an algorithm that is both fast and capable of providing images with adequate spatial resolution. The thoracic shape can contribute as much as the internal thoracic impedances towards the voltages picked up on the chest wall surface. Consequently, reconstruction of absolute impedance distribution, although feasible, requires knowledge regarding chest shape (9). To avoid taking thoracic geometry into account, Sinton *et al.* suggested an approach based on dynamic impedance changes, that is, relative changes in impedance for certain times or during respiration, assuming that the shape of the chest did not change between measurements (10).

To grasp the complexity of the reconstruction algorithms, it is useful to compare EIT to computed tomography (CT) using X-rays. The reconstruction of a CT image is relatively simple because the X-rays cross the chest in a straight line, with negligible energy scatter. Therefore, a localized change in tissue density only affects measurements taken by the detectors on the projection of the line connecting to the X-ray projector. The electric current, however, passes through the chest by dispersing into three dimensions following a complex distribution that is determined by the current injection site as well as by the three-dimensional impedance distribution characteristics (9,10).

The *Sheffield backprojection algorithm* assumes a rounded shape of the axial section of the thorax, thus they introduce *a priori* information in the representation of the data. The bioimpedance measurements can be classified into two types. The first type implies a reduction in the observed impedance, as is the case in tissues that have an increase in the extracellular water content, a high concentration of electrolytes and a high number of cell junctions. The second type implies an increase in impedance, as occurs with fat, bone and air, which act as resisting elements. Thus, reconstruction—based on changes in impedance that are compared to a reference (giving it the name of relative impedance)—is used, since it is assumed that the shape of the chest does not change between the two (9).

An important aspect to consider is that reconstruction algorithms rule out measurements from poorly positioned electrodes and ignore redundant data, which implies making assumptions regarding the level of interference with *raw data* (unprocessed data). There is also variance depending on the algorithm used by the manufacturer: Sheffield

backprojection (used by Goe-MF II and Mark 1 and Mark 3.5), Finite Element Method (FEM) based Newton-Raphson (used by PulmoVista and Enlight) and GREIT (used by BB®) (11).

The change in thoracic bioimpedance is influenced fundamentally by two cyclical mechanisms: ventilation and perfusion. The increase in the amount of air during inspiration—coupled with the increase in lung volume and the change in rib cage volume—leads to an increase in impedance that is proportional to the volume of inspired gas. On the other hand, pulmonary perfusion leads to small changes—of the order of 3%—in the thoracic impedance between systole and diastole.

Ventilation monitoring

During quiet breathing, lung tissue impedance changes by around 5%, while in deep breathing it can reach up to 300% (from the residual volume up to the total lung capacity). As mentioned, the increase in the amount of air during inspiration leads to proportional increases in impedance (a decrease in current conductivity) in such a manner that if we associate the impedance meter with volume measurements administered by the ventilator, we can get it to behave like a true plethysmograph, furthermore incorporating the respiratory flow, airway pressures, and compliance (12). Then, the study of the changes in relative impedance allows the estimation of the tidal volume, the percentages of the tidal volume distribution in each region of interest (ROI) (selecting quadrants or layers), the minimum impedance (end-expiratory lung impedance) or maximum impedance (total lung capacity). In other words, EIT allows observing the distribution of the gas volume entering the lung (in the sectional plane, 5th intercostal space) and to evaluate the regional characteristics of pulmonary structure, which is why it can be considered as an ideal tool for monitoring typical pulmonary heterogeneity in ARDS as well as for guiding the modification of PEEP and tidal volume, which contributes toward the prevention of ventilator-induced lung injury (13). The EIT has also been used as a monitoring method in non-conventional modes of mechanical ventilation, such as in high frequency ventilation (14).

The reconstruction of the images calculates the changes in the properties of the lung tissue between a frame obtained basally with another current one. These time-difference images are adapted in order to pick up physiological phenomena that vary over time, such as lung ventilation and perfusion. The electrodes should also bear low sensitivity to the movements of the signal contour. In the images obtained with the most up to date algorithms, the contour reflects the anatomical shape of the thorax. Breakthroughs in imaging quality have been attained through the use of *a priori* anatomical information, for example, through those obtained from CT (2).

The EIT for measurement of regional lung volume distribution has also been validated upon comparison to positron emission tomography (PET) (15), computed tomography (4) and MRI (16); both on animal models and on humans (with healthy and injured lungs), independently of severity of lung damage or whether breathing was spontaneous or mechanically delivered [over a wide range of PEEP and tidal volume (VT)].

Perfusion monitoring

The quantification of pulmonary perfusion by EIT can be performed by a brief respiratory pause, followed by rapid infusion of hypertonic saline, which will dramatically reduce chest impedance, thus acting as an intravascular contrast (*Figure 3*). Pulmonary perfusion by EIT proved to be capable of producing significant and well-agreed V/Q maps as compared to perfusion maps produced using single photon emission tomography (SPECT) (17). Another possibility is based on the separation of the cardiac signal from the ventilation signal through electrocardiogram gating or through the principal component analysis (PCA) (18).

Clinical applications

In the beginning, the applications of EIT were aimed mainly at determining changes in pulmonary ventilation distribution. Nevertheless, at the moment there are studies aimed at the evaluation of lung recruitment/collapse or derecruitment/overdistention, the detection of pneumothorax, lung perfusion, EIT-guided fluid management and assessment of cardiac function in the critical care setting.

Collapse, overdistension and EIT-guided PEEP titration

The main available tools for evaluation of pulmonary mechanics have been the use of P-V curve and the measurement of static compliance, however, these are incapable of accounting for what happens in the lung at the regional level. It is also possible to monitor the behavior of

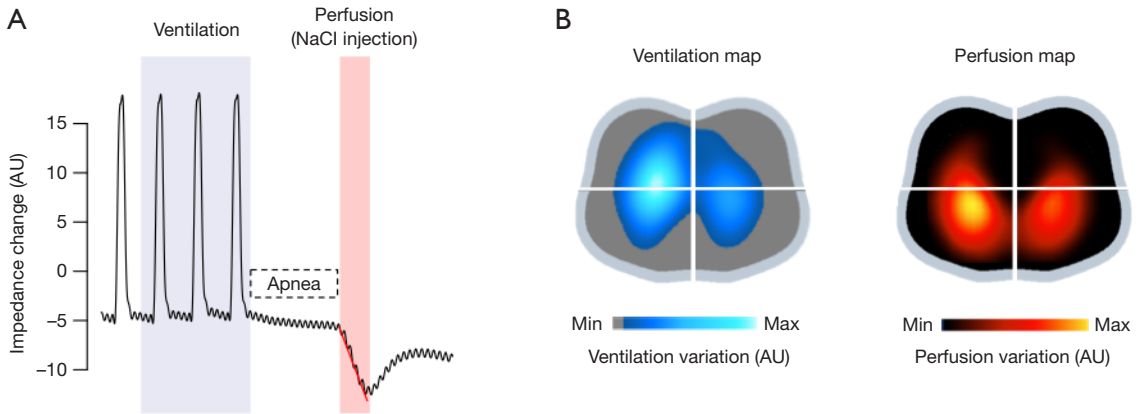

Figure 3 Shows in (A) the maximum slope of impedance reduction upon injecting of 10 mL 7.5% NaCl (the period that indicates the passage of the indicator through the lung territory), and in (B) the map of ventilation and perfusion obtained with Electrical Impedance Tomography Enlight 1800 (Timpel, Sao Paulo, Brazil). Using saline injection in a patient with pneumonia in the left lower lobe. In this case, the limited perfusion and ventilation of the left lung can be observed. Combined with other patient exams, this bedside information may facilitate the understanding of the clinical scenario and guide the medical intervention.

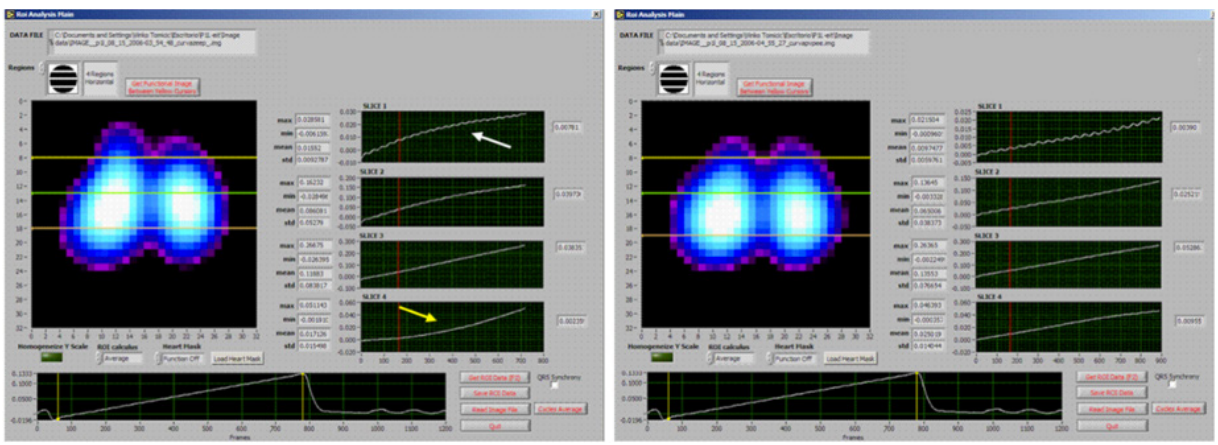

Figure 4 Curve demonstrating quasi-static inflation with a flow of 1 L/min in a focal ARDS model. Each window corresponds to the respective region of interest (ROI) or layer of each analyzed image. On the left graph, a Pressure-Volume curve obtained with 15 cmH_2O positive end-expiratory pressure (PEEP) without recruitment is observed. In the first window there is a lower concavity showing the upper inflection point (UIP) (white arrow) and in the 4th window there is an upper concavity representing lower inflection point (LIP) (yellow arrow). On the right, you can see a Pressure-Volume curve from post-recruitment 15 cmH_2O PEEP (40 cmH_2O for 40 seconds) where alignment of the curve can be seen in the four windows (suppression of UIP and LIP). The lower graphs in both images—right and left—demonstrate slow flow inflation. Swine model presenting focal ARDS from serial single-lung bronchoalveolar lavage with warm saline. Dr. Vinko Tomicic Medical Research Laboratory (LIM 09). University of Sao Paulo, Brazil, 2006. ARDS, acute respiratory distress syndrome.

the regions (*layers*) during the inspiratory P-V curve before and after a lung recruitment maneuver by observing the suppression of the phase lag presents in the lower layer of the pre-recruitment curve versus the post-recruitment curve (*Figure 4*). As collapse and overdistension may coexist during mechanical ventilation, it is necessary to have a tool that makes it possible to discern the presence of both. This is how—thanks to clinical incorporation of EIT—it is now possible to determine both phenomena simultaneously. It is also possible to quantify aeration gain (recruitment) and

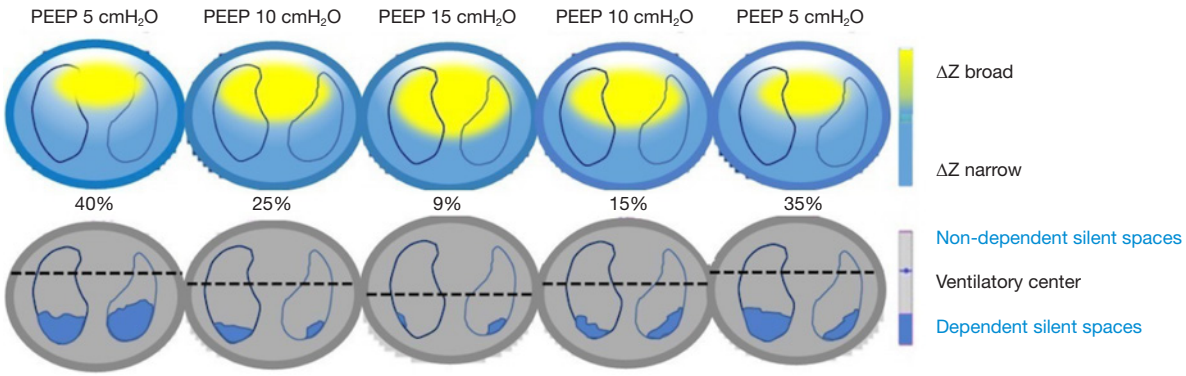

Figure 5 Modified from Spadaro *et al.* (23): top in blue: regional impedance maps (ΔZ) with different levels of positive end-expiratory pressure (PEEP) (ascending 5, 10 and 15 cmH_2O and descending 10 and 5 cmH_2O). In the lower figures, the black dotted line shows the centralization of the ventilation by increasing the PEEP (recruitment); along with that, there is a reduction in the dependent silent spaces (blue), which reappear with PEEP decrease. In the same color one can observe the percentages of the dependent silent zones located above the sequencing of figures. Although marginal, there are silent spaces in the non-dependent region.

aeration losses, which can occur in cases of overdistention or in cases of de-recruitment, guaranteeing a more objective evaluation of the different ventilatory modes, lung recruitment maneuver as well as aiding in the identification of responders and non-responders to such maneuvers (19,20). The rationale is based on the estimation of the regional compliances using functional imaging, combined with airway pressures. Thus, the changes in pixel compliance during a decremental PEEP trial can be used to define collapse and overdistension by pixel, and consequently by any region of interest (2,21,22), By employing PEEP titration based on EIT, better respiratory mechanics and balance between overdistension and collapsed are achieved (*Figures 4*,*5*).

Though careful PEEP titration is important, one should keep in mind that pulmonary condition is constantly changing (due to intra-abdominal pressure, changes in position, aspiration of secretions, etc.) and that the selected PEEP does not keep the lung open at all times, especially upon airway depressurization. Data obtained from most of the studies suggest that changes in relative impedance measured by EIT can be used to quantify regional ventilation with enough precision in adults and pediatric population (2). In this sense, continuous EIT monitoring is a useful tool for detecting these potential variations in pulmonary aeration. In addition, some patients with severe respiratory failure may develop predominant overdistension with higher levels of PEEP (for example lobar ARDS), which may be detected through EIT monitoring; these non-recruiter patients should be managed with other alternative therapies like prone positioning or extracorporeal membrane oxygenation (ECMO). EIT monitoring can also be maintained in prone and ECMO (*Figure 6*), although evidence for its use is lacking. If the patients are stable hemodynamically and the airway pressure used during recruitment maneuvers is up until 45 cm of water (performed in steps), better hemodynamic tolerance is observed (24,25); higher airway pressures and hemodynamic instability should be avoided.

Employing EIT during PEEP titration in patients with higher lung collapse, but without significant non-aerated areas (*Figures 5*,*7*, patient B), it is possible to observe PEEP-induced changes in EIT-derived poorly ventilated areas, mainly in the dependent lungs, which are correlated with recruitment determined by the P-V curve. In the same line, the decrease on EIT-derived poorly ventilated areas has been associated with better regional compliance of the dependent lung areas (23).

Recruitment monitoring with EIT

In an animal model, Costa *et al.* compared the alveolar collapse obtained by CT and EIT at the same time and found a good correlation between both methods during a maximum lung recruitment maneuver and decremental PEEP titration. In *Figure 8*, a PEEP titration from one of our patients is shown.

However, we should keep in mind that collapse detected by EIT during PEEP titration trial is the accumulated collapse after a recruitment maneuver. It is very close to

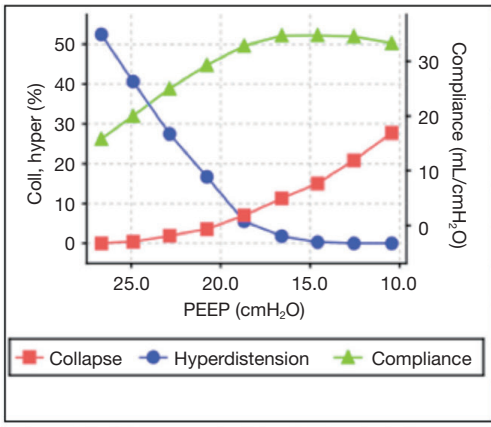

PEEP (cmH_2O)	Compliance (mL/cmH_2O)	Hyperdis-tension (%)	Collapse (%)
26.7	15.8	52.4	0.0
24.9	20.0	40.6	0.4
22.9	25.0	27.5	1.9
20.8	29.3	16.7	3.6
18.7	32.8	5.6	7.0
16.6	34.7	1.8	11.3
14.6	34.7	0.3	15.1
12.6	34.5	0.0	20.8
10.4	33.3	0.0	27.7

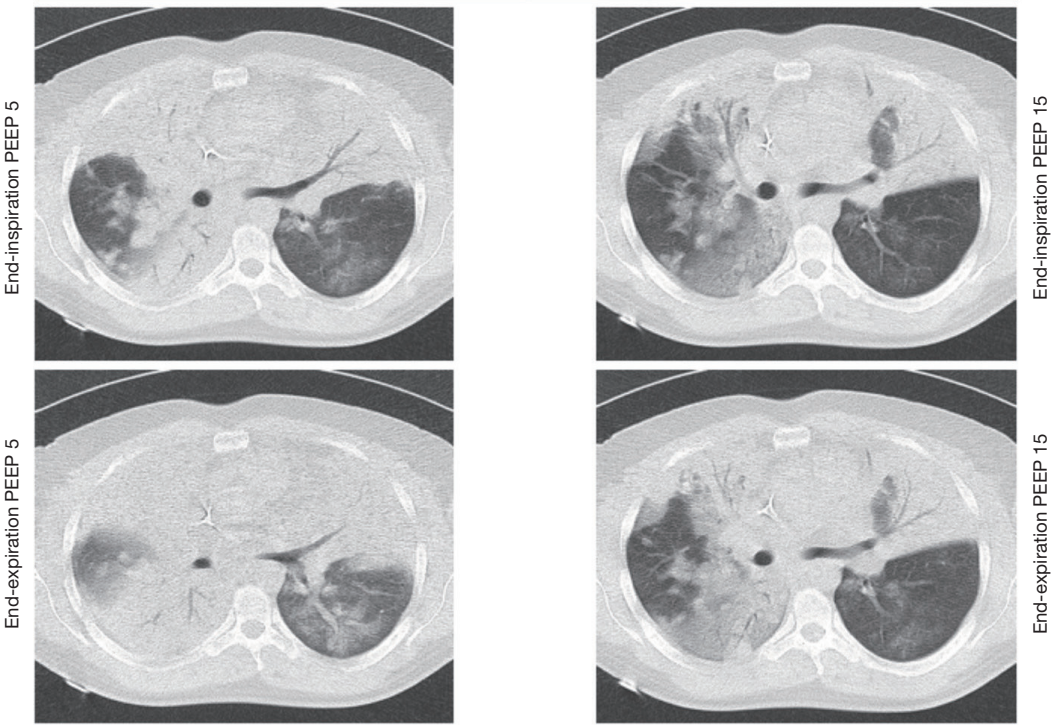

Figure 6 Computed tomography (CT) and electrical impedance tomography (EIT) assessments in an ARDS patient in prone positioning. On the top, there is a positive end-expiratory pressure (PEEP) titration according EIT. On the bottom, there are CT slices taken at end-expiratory and end-inspiratory with PEEP 5 and PEEP 15 cmH_2O. In this patient with highly recruitable lung, the use of PEEP 15 was associated to better respiratory mechanics (higher compliance and lower driving pressure), and higher recruitment and lower tidal recruitment/derecruitment in comparison with PEEP 5. ARDS, acute respiratory distress syndrome.

potentially recruitable lung defined by CT, also after a recruitment maneuver, but it may differ from non-aerated regions for a given level of PEEP, because non-aerated regions may be composed by alveolar collapse, fluid-filled alveolus and consolidation (*Figure* 7).

Frerichs *et al.* induced acute lung injury in 16 swine models with the pulmonary lavage technique and demonstrated that EIT was able to display the harmful effects of pulmonary lavage, lung recruitment, administration of surfactant and ventilatory techniques used thereafter. They found that lung injury displaces ventilation ventrally and lung recruitment maneuver can restore the ventilation center to normal values (*upper and lower* ratio~1) (12).

Muders *et al.* compared EIT to dynamic CT in 18

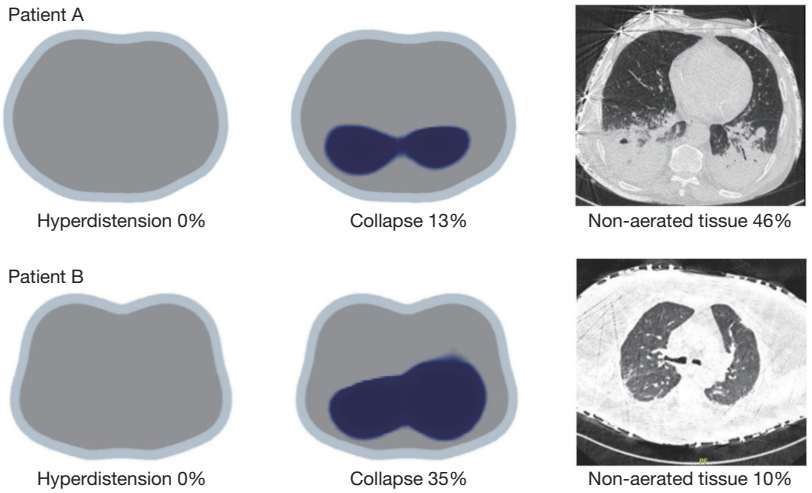

Figure 7 Simultaneous acquisitions of computed tomography (CT) and electrical impedance tomography (EIT) images (Enlight, Timpel, Sao Paulo, Brazil) at positive end-expiratory pressure (PEEP) 5 cmH_2O, after performing a recruitment maneuver and PEEP decremental trial. Patient A has 13% of collapse, but 46% of non-aerated region, while Patient B (morbidly obese) has 35% of collapse, but only 10% of non-aerated region. In both cases, overdistension was 0% at PEEP 5 cmH_2O. Effectively, in the Patient A when comparing the CT at PEEP 5 cmH_2O with CT images taken at 45 cmH_2O (not shown), we observed a percentage of potentially recruitable lung of 12%. In the other hand, Patient B could be related to "silent spaces", which is only found using EIT monitoring or transpulmonary pressure at end expiration. Project FONDECYT 1161510. Cornejo *et al.*

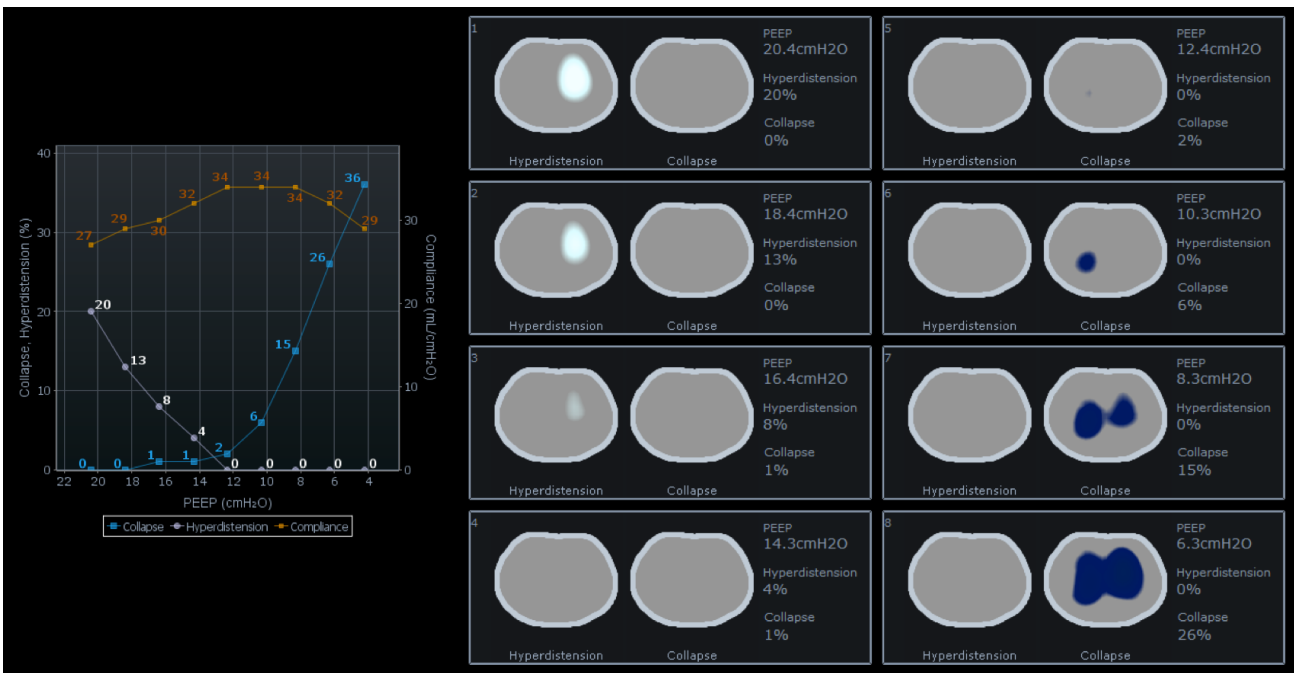

Figure 8 Decremental PEEP titration trial after performing a maximum recruitment maneuver, employing electrical impedance tomography monitoring. The pixels in white describes the overdistension, which dissipates as positive end-expiratory pressure (PEEP) decreases, until disappearing with a PEEP of 12 cmH_2O. In blue, the beginning of the collapse can be observed (from PEEP 16). With a PEEP of 12 the overdistension (light blue) has disappeared and there are low levels of collapse [blue]. At PEEP 13, there would be a balance between the two conditions; this is considered the best imaging step to titrate PEEP, which coincides with best compliance. This image is provided by Enlight 1800, Timpel, Sao Paulo, Brazil. Project FONDECYT 1161510. Cornejo *et al.*

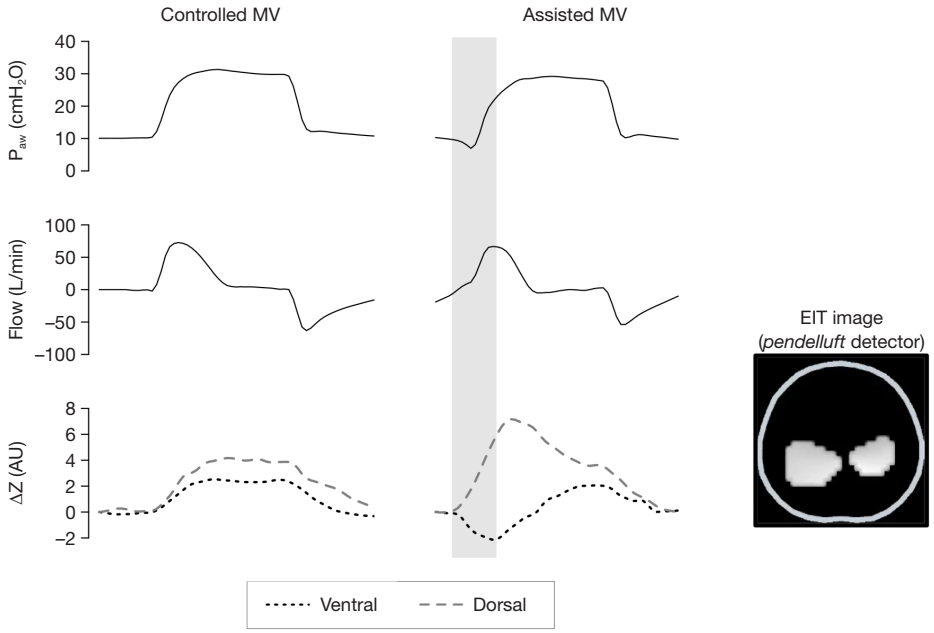

Figure 9 Pendelluft phenomenon detected by electrical impedance tomography Enlight 1800. In Controlled mechanical ventilation, the magnitude of relative impedance changes at ventral and dorsal regions are similar during a respiratory cycle. However, in Assisted mechanical ventilation, some patients may experience pendelluft, that is, displacement of gas from ventral (more recruited regions) to dorsal lung (less recruited regions) during early inspiration. This as a consequence of strong contractions of the diaphragm, generating high distending forces, which are concentrated in dorsal lung regions (12).

swine models that were divided into three groups (control, direct and indirect lung injury groups). During a slow inflation maneuver, they measured the regional impedance versus time and calculated 3 indexes: area below the curve, slope linearity and lag between the start of inspiration and the start of the regional image inflation (ventilatory lag index). They demonstrated that recruitment could be detected and that the ventilatory lag index best described the regional recruitment. In addition, it was observed that the recruitment produced during the insufflation could be detected (*intra-tidal recruitment*) (26).

Regional expiratory time constants assessed by EIT

Recently, Karagiannidis *et al.* provided a new promising EIT tool assessing regional expiratory time constants in patients with obstructive pulmonary diseases and ARDS (27). The authors found that expiratory time constants calculated from the global impedance EIT signal [based on the equation: $V(t) = Vo*e^{-t/\tau} + C$, where V(t) is the volume at that time point t, Vo is the volume at the start of expiration, t the time from the start at end-inspiration to the end of expiration, τ the expiratory time constant and C the end-expiratory volume] were accurately compared to the pneumatic volume signals measured with an electronic pneumotachograph, which may help to guide mechanical ventilation in response to the patterns of regional airflow obstruction.

Pendelluft phenomenon detected by EIT

During spontaneous breathing, the capability of EIT to monitor imbalances in regional lung ventilation allows detection of pendelluft phenomenon (*Figure 9*).

Pendelluft is an intrapulmonary dyssynchrony characterized by gas exchange between different lung regions. Through the EIT, Yoshida *et al.* described excessive alveoli stretching in the dorsal region (severity dependent) during assisted mechanical ventilation, without any signs of irregularities in the ventilator curves (28). Recently, Morais *et al.* showed worsening of pulmonary inflammation associated with local volutrauma caused by pendelluft, especially in regions close to the diaphragm (29). Therefore, EIT could help guide the ventilatory

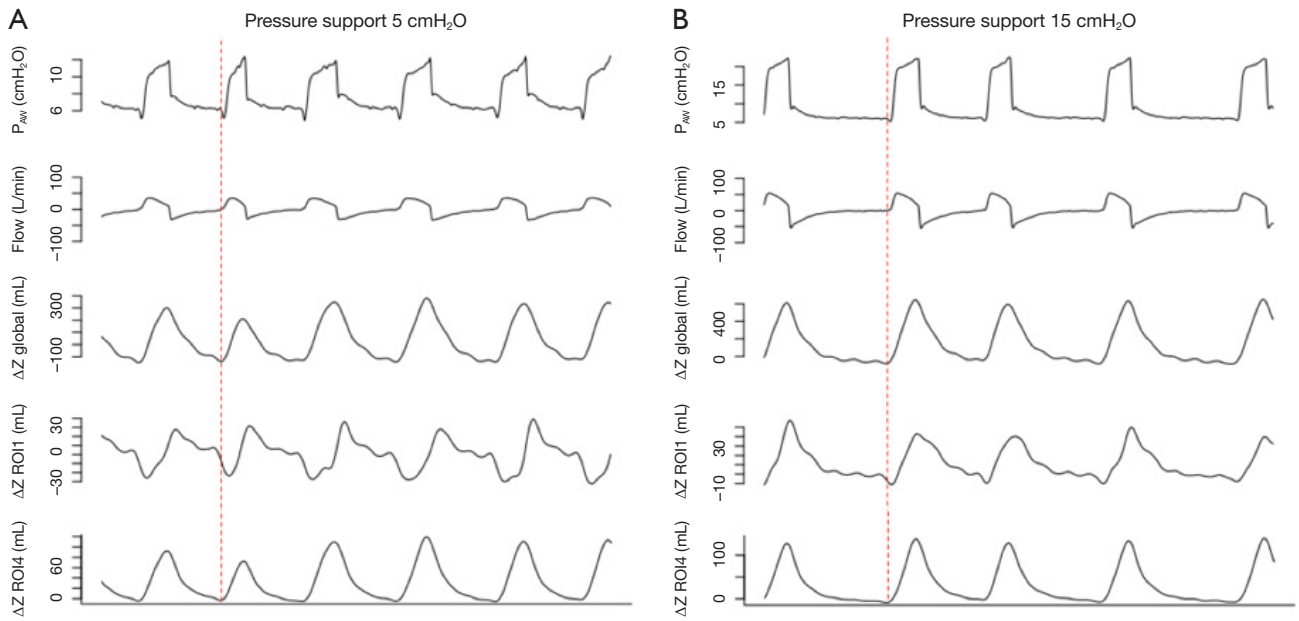

Figure 10 There are two graphs from an ARDS patient under spontaneous breathing in pressure support ventilation and "best" positive end-expiratory pressure (PEEP) set according electrical impedance tomography (EIT), with two levels of pressure support (PS). In (A) the level of PS is 5 cmH_2O, and in (B), PS is 15 cmH_2O. Time is on the x-axis and different parameters [airway pressure: Paw, respiratory flow: Flow, and tidal impedance, global and by region of interest (ROI) are on the y-axis. In this particular case, EIT monitoring shows that pendelluft phenomenon (differences between ROI 1 "ventral region" and ROI 4 "dorsal region"), evident with PS 5, practically disappeared with PS 15 (Project FONDECYT 1161510. Cornejo *et al.*]. ARDS, acute respiratory distress syndrome.

settings focusing on respiratory mechanics, synchrony and pendelluft during different spontaneous breathing modes, such as pressure support ventilation (*Figure 10*), proportional assist ventilation, neurally adjusted ventilatory assist or airway pressure release ventilation.

Detection of pneumothorax and EIT-guided fluid management

An interesting and new diagnostic tool provided by EIT was developed for the detection of pneumothorax; less than 50 mL in less than 5 respiratory cycles can be detected with sensitivity of 100%. This early and accuracy diagnosis is obtained due to the large changes in the aeration maps caused by small volumes of air in the pleural space. The detection algorithm is based on the perturbations generated by the pneumothorax using two criteria: decrease in regional ventilation and asymmetry (30).

EIT has been explored for stroke volume estimation, although it will never achieve outstanding accuracy and requires more research (31). However, the ability of systolic impedance variations (ΔZsys) to track changes in stoke volume was recently studied. Interestingly, Da Silva *et al.* showed that changes in ΔZsys can potentially substitute changes in stroke volume in the assessment of fluid responsiveness, relationship which was not influenced by changes in PEEP or VT (32), offering new prospects for EIT development.

Technical limitations

With EIT it is only possible to obtain impedance images of an axial section of the chest (5 to 10 cm high), leaving out the rest of the lung parenchyma. On the other hand, the spatial resolution of the technique—both in terms of ventilation (each pixel contains information on the impedance of many alveolar units) and perfusion—remains low. Besides, we have yet to confirm that EIT provides functional and non-anatomical images of the portion of evaluated tissue (2).

The EIT images translate changes in the impedance of lung tissue, and not absolute values. Therefore, the pre-monitoring conditions, such as consolidation or pleural effusions, cannot be identified. In 25 ventilated patients

with different levels of PEEP, Bikker *et al.* attempted to correlate the end-expiratory lung volume (EELV) with the end-expiratory lung impedance (EELI) and concluded that the linear relationship between changes in volume and impedance does not make it possible to determine end-expiratory lung volume (which is an absolute value, not a change). Another weakness is the calibration of the system. As it is the case regarding all techniques, it is fundamental to associate the changes exhibited by EIT with the clinical and radiological changes observed in the patient (33,34).

Overcoming the limitations of EIT

Applying greater currents to the electrodes would also increase the image resolution by reducing the effects of contact impedance, yet this is not the case for the composite electrodes. In this mechanism, the adjacent method protocol was used to collect the data. This is because, when applying EIT method, independent impedance measurements can be obtained. As such, in the next data acquisition process, there will be 20 available impedance measurements. By having these additional independent impedances, the reconstructed image could undoubtedly achieve a higher resolution compared to other images produced by conventional EIT systems (2). Special electrodes featuring capacitive noise reduction were also designed to improve image resolution: (I) inflatable belt; (II) active electrode belt; (III) nanofiber band electrode belt (2). Gaggero *et al.* developed an active electrode EIT system in which each active electrode comes with its own signal conditioning circuit, which reduces input impedance, thus contributing to better image resolution. However, this belt can be used for a single study. The parasitic capacitance from the cables can be reduced by situating the signal conditioning circuit near the active electrodes (35). Similarly, a flexible belt was designed by Sohal *et al.* (36).

Conclusions

As one of the main methods able to assess lung function non-invasively and at the bedside, the EIT will certainly have growing role in intensive care medicine, assisting clinical decision making. New clinical tools that will be available in the EIT can help optimize mechanical ventilation aids, detect complications such as ventilatory dyssynchrony, pulmonary disarticulation, and pneumothorax, and provide maps of lung ventilation and perfusion. Although EIT seems to be a promissory tool for non-invasive radiation free monitoring at bedside in the critical care scenario, further studies are needed to demonstrate its impact on clinical outcomes.

Acknowledgments

Funding: This work was supported by a grant of Fondo Nacional de Desarrollo Científico y Tecnológico (FONDECYT) Nº 1161510, Gobierno de Chile.

Footnote

Conflicts of Interest: The authors have no conflicts of interest to declare.

Ethical Statement: The authors are accountable for all aspects of the work in ensuring that questions related to the accuracy or integrity of any part of the work are appropriately investigated and resolved.

References

1. Chiumello D, Froio S, Bouhemad B, et al. Clinical review: Lung imaging in acute respiratory distress syndrome patients - an update. Critical Care 2013;17:243.
2. Frerichs I, Amato M, van Kaam A, et al. Chest electrical impedance tomography examination, data analysis, terminology, clinical use and recommendations: consensus statement of the TRanslational EIT developmeNt stuDy group. Thorax 2017;72:83-93.
3. Costa EL, Gonzalez R, Amato MB. Electrical impedance tomography. Curr Opin Crit Care 2009;15:18-24.
4. Victorino JA, Borges JB, Okamoto VN, et al. Imbalances in regional lung ventilation: a validation study on electrical impedance tomography. Am J Respir Crit Care Med 2004;169:791-800.
5. Riera J, Riu PJ, Casan P, et al. Tomografía de impedancia eléctrica en la lesión pulmonar aguda. Medicina Intensiva 2011;35:509-17.
6. Wrigge H, Zinserling J, Muders T, et al. Electrical impedance tomography compared with thoracic computed tomography during a slow inflation maneuver in experimental models of lung injury. Crit Care Med 2008;36:903-9
7. Luepschen H, Meier T, Grossherr M, et al. Protective ventilation using electrical impedance tomography. Physiol Meas 2007;28:S247-60.
8. Yorkey TJ, Webster JG, Tompkins WJ. Comparing

Reconstruction Algorithms for Electrical Impedance Tomography. IEEE Trans Biomed Eng 1987;34:843-52.
9. Lionheart WR. EIT reconstruction algorithms: pitfalls, challenges and recent developments. Physiol Meas 2004;25:125-42.
10. Sinton AM, Brown BH, Barber DC, et al. Noise and spatial resolution of a real-time electrical impedance tomograph. Clin Phys Physiol Meas 1992;13 Suppl A:125-30.
11. Lobo B, Hermosa C, Abella A, et al. Electrical impedance tomography. Ann Transl Med 2018;6:26-35.
12. Frerichs I, Dargaville PA, van Genderingen H, et al. Lung volume recruitment after surfactant administration modifies spatial distribution of ventilation. Am J Respir Crit Care Med 2006;174:772-9.
13. Hinz J, Gehoff A, Moerer O, et al. Regional filling characteristics of the lungs in mechanically ventilated patients with acute lung injury. Eur J Anaesthesiol 2007;24:414-24.
14. van Heerde M, Roubik K, Kopelent V, et al. Spontaneous breathing during high-frequency oscillatory ventilation improves regional lung characteristics in experimental lung injury. Acta Anaesthesiol Scand 2010;54:1248-56.
15. Richard JC, Pouzot C, Gros A, et al. Electrical impedance tomography compared to positron emission tomography for the measurement of regional lung ventilation: an experimental study. Critical Care 2009;13:R82.
16. Dunster KR, Friese ME, Fraser JF, et al. Ventilation distribution in rats: Part 2--A comparison of electrical impedance tomography and hyperpolarised helium magnetic resonance imaging. Biomed Eng Online 2012;11:68.
17. Borges JB, Suarez-Sipmann F, Bohm SH, et al. Regional lung perfusión estimated by electrical impedance tomography in a piglet model of lung collapse. J Appl Physiol 2012;112:225-36.
18. Ericsson E, Tesselaar E, Sjöberg F. Effect of Electrode Belt and Body Positions on Regional Pulmonary Ventilation- and Perfusion-Related Impedance Changes Measured by Electric Impedance Tomography. PLoS One 2016;11:e0155913.
19. Wolf GK, Grychtol B, Frerichs I, et al. Regional lung volume changes in children with acute respiratory distress syndrome during a derecruitment maneuver. Crit Care Med 2007;35:1972-8.
20. Frerichs I, Hahn G, Schiffmann H, et al. Monitoring regional lung ventilation by functional electrical impedance tomography during assisted ventilation. Ann NY Acad Sci 1999;873:493-505.
21. Costa ELV, Borges JB, Melo A, et al. Bedside estimation of recruitable alveolar collapse and hyperdistension by electrical impedance tomography. Intensive Care Med 2009;35:1132-7.
22. Liu S, Tan L, Möller K, et al. Identification of regional overdistension, recruitment and cyclic alveolar collapse with electrical impedance tomography in an experimental ARDS model. Critical Care 2016;20:119.
23. Spadaro S, Mauri T, Böhm S, et al. Variation of poorly ventilated lung units (silent spaces) measured by electrical impedance tomography to dynamically assess recruitment. Critical Care 2018;22:26.
24. Gattinoni L, Caironi P, Cressoni M, et al. Lung recruitment in patients with the acute respiratory distress syndrome. Lung recruitment in patients with the acute respiratory distress syndrome. N Engl J Med 2006;354:1775-86.
25. Kacmarek RM, Villar J, Sulemanji D, et al. Open lung approach for the acute respiratory distress syndrome. Crit Care Med 2016;44:32-42.
26. Muders T, Luepschen H, Zinserling J, et al. Tidal recruitment assessed by electrical impedance tomography and computed tomography in a porcine model of lung injury. Crit Care Med 2012;40:903-11.
27. Karagiannidis C, Waldmann A, Róka P, et al. Regional expiratory time constants in severe respiratory failure estimated by electrical impedance tomography: a feasibility study. Critical Care 2018;22:221.
28. Yoshida T, Torsani V, Gomes S, et al. Spontaneous effort causes occult pendelluft during mechanical ventilation. Am J Respir Crit Care Med 2013;188:1420-7.
29. Morais CCA, Koyama Y, Yoshida T, et al. High Positive End-Expiratory Pressure Renders Spontaneous Effort Noninjurious. Am J Respir Crit Care Med 2018;197:1285-96.
30. Costa EL, Chaves CN, Gomes S, et al. Real-time detection of pneumothorax using electrical impedance tomography. Crit Care Med 2008;36:1230-8.
31. Pikkemaat R, Lundin S, Stenqvist O, et al. Recent Advances in and Limitations of Cardiac Output Monitoring by Means of Electrical Impedance Tomography. Anesth Analg 2014;119:76-83.
32. da Silva Ramos FJ, Hovnanian A, Souza R, et al. Estimation of Stroke Volume and Stroke Volume Changes by Electrical Impedance Tomography. Anesth Analg 2018;126:102-10.
33. Bikker IG, Leonhardt S, Reis Miranda D, et al. Bedside

measurement of changes in lung impedance to monitor alveolar ventilation in dependent and non-dependent parts by electrical impedance tomography during a positive end-expiratory pressure trial in mechanically ventilated intensive care unit patients. Crit Care 2010;14:R100.
34. Costa ELV, Gonzalez Lima R, Amato MBP. Electrical Impedance Tomography. Year Book of Intensive Care and Emergency Medicine. Edited by JL Vincent Editorial. Springer Verlag, 2009:394-404.
35. Gaggero PO, Adler A, Brunner J, et al. Electrical impedance tomography system based on active electrodes. Physiol Meas 2012;33:831-47.
36. Sohal H, Wi H, McEwan AL, et al. Electrical impedance imaging system using FPGAs for flexibility and interoperability. Biomed Eng Online 2014;13:126.

Cite this article as: Tomicic V, Cornejo R. Lung monitoring with electrical impedance tomography: technical considerations and clinical applications. J Thorac Dis 2019;11(7):3122-3135. doi: 10.21037/jtd.2019.06.27

